DOI: https://doi.org/10.37434/tpwj2024.12.03

FORMATION OF POROUS COATINGS ON TITANIUM ALLOYS BY THE METHOD OF PLASMA ELECTROLYTIC OXIDATION IN ALKALINE ELECTROLYTES SATURATED WITH PHOSPHATES AND BIO-ADDITIVES

N.Yu. Imbirovych[1], **O.Yu. Povstyanoy**[1], **K.J. Kurdzydlowski**[2], **V.V. Tkachuk**[1]

[1]Lutsk National Technical University
75 Lvivska Str., 43018, Lutsk, Ukraine. E-mail: n.imbirovych@lntu.edu.ua
[2]Bialystok University of Technology
45A, Wiejska Str., 15-351 Bialystok, Poland

ABSTRACT

Environmentally friendly electrolytes have been developed to ensure the formation of coatings based on titanium alloys by plasma electrolytic processing, which contain phosphates in the form of sodium pyrophosphate ($Na_4P_2O_7$) and sodium hexamethophosphate ($Na_6P_6O_{18}$), calcium-containing components in the form of calcium hydroxide and hydroxylapatite, as well as a bio-additive in the form of diatomite in different concentrations. The study of the stages of PEO coating formation is presented with the help of time dependences of the voltage change on the anode during the processing. The presented dependencies made it possible to establish the optimal ratio of I_a/I_c current density, at which uniform coatings are formed. The through-thickness porosity of the synthesized PEO-coatings in different modes was determined through experimental studies. It is shown that coatings formed in an electrolyte with phosphates are characterized by the maximum rate of such porosity (0.75 %), while high water absorption is characteristic of coatings formed in an electrolyte with diatomite, which is 1.21 % against 0.6 %. Such values satisfy the conditions of biocompatibility of the materials.

KEYWORDS: plasma electrolytic oxidation; synthesis, biocompatibility, coating, porosity, thickness

INTRODUCTION

Plasma electrolytic oxidation (PEO), also known as microarc oxidation (MAO) or anode spark deposition (ASD), is a cost effective and ecofriendly technology, which allows forming an oxide on the surface of aluminium, magnesium, titanium, zirconium, tantalum, niobium, hafnium and other light metals and their alloys [1–5]. More over, the thus formed oxide coatings are characterized by a controlled morphology, high microhardness, wear- and corrosion resistance, excellent strength of adhesion to the base, high dielectric and thermal properties [6–14].

During PEO discrete spark discharges appear on the surface, when the applied voltage exceeds the critical values (known as the voltage of breakdown of the oxide semiconductor film). The discharge occurs as a result of the loss of the oxide film dielectric stability in the low electric conductivity region. This process is accompanied by sparking [15] and gas evolution [16, 17]. The microdischarge leads to high temperature and pressure in the local region that allows forming oxide coatings, which consist not only of the stoichiometric composition of the processed metal oxides, but also from more complex oxides, containing compounds, which form as a result of plasma-chemical reactions of the metal with the electrolyte components [18]. Although the microdischarge phenomena and their influence on the formation mechanism, composition, morphology and other properties of oxide PEO-coatings on aluminium and magnesium have been sufficiently researched, the correlated studies of titanium have not been fully conducted.

Titanium is a widely used metal in engineering, owing to its properties, such as high strength, low density, high melting temperature and good biocompatibility [19–21]. The effectiveness of using titanium alloys in implantology was studied for a long time [22, 23]. The high biocompatibility is due to titanium ability to form on its surface a protective oxide layer in fractions of a second, due to which it does not corrode and does not release free metal ions, which can cause pathological processes in the vicinity of the implant. Due to that, the tissues adjacent to the prosthesis remain free from metal ions [24].

Titanium alloys are used as prosthesis of shoulder, hip and knee joints, as well as for manufacturing plates for fracture splicing. Titanium lightness also determines its wide application for medical instruments [25, 26]. However, after bone replacement surgery, at least 17.5 % of the cases require repeated operation [27]. Incomplete osteointegration and bacterial infection are a threat for normal implant survival. The authors of [28] describe effective application of coatings with a wide porosity range in their work. This effect leads to higher osteointegration [29].

It is known that the main disadvantages of the titanium alloys are poor machinability, high coefficient of friction, relatively low modulus of elasticity, while a low chemical activity and strength of adhesion to the muscle tissues and the bone are also added for implantology. These facts can lead to resorption of the bones in their vicinity [30, 31].

An efficient method to prevent this effect is predeposition of a bactericidal layer on the material surface. Arash Fattah-alhosseini et al. report that a lot of attention should be given to coating nontoxicity that may lead to appearance of multidistant pathogens [32, 33]. A possible solution to this problem is surface modifications which improve the implant osteointegration, or reduce the bacterial infection. In view of the above, application of compositions with antimicrobial properties in the bone plastics is promising [34, 35]. These are exactly the requirements satisfied by PEO as a promising method with the possibility of modification of the light alloy surface with various calcium-containing components, phosphates and bio-additives [36–39].

THE OBJECTIVE

of this work is development of the technology of saturation of oxide PEO-coatings based on a titanium alloy with phosphates and diatomaceous soil (diatomite) to increase their porosity and roughness.

INVESTIGATION PROCEDURE

The object of study are coatings based on Ti–6Al–4V titanium alloy (class 5), which was synthesized by the method of plasma electrolytic oxidation. Round flat samples of the following dimensions: 20 mm diameter, 5 mm thickness were tested. The electrolyte was an aqueous solution based on potassium hydroxide (KOH), calcium hydroxide ($Ca(OH)_2$), sodium silicate ($Na_2O(SiO_2)_n$), sodium pyrophosphate ($Na_4P_2O_7$), sodium hexamethophosphate ($Na_6P_6O_{18}$) at their different concentration (0.5–20 g/l). To clarify the influence of bioactive natural materials on the coating properties, calcium hydroxylapathite ($Ca_{10}(PO_4)_6(OH)_2$) and diatomite (main component is SiO_2) were added to the electrolyte in the amount of 1 and 20 g/l, respectively. PEO modes were characterized by the ratio of the anode to cathode currents, I_a and I_c, respectively, and by processing duration.

In this work we considered the characteristics of a microdischarge at plasma electrolytic oxidation through determination of electrophysical parameters of the coating synthesis. Coating morphology was studied in Tagarno Prestige FHD microscope, Xplus controller and 3D laser scanning microscope Keyence VHX 7000. Coating roughness was analyzed in keeping with DSTU ISO 4287:2012 by the following parameters: R_a — arithmetic mean deviation of the profile, R_z — height of profile unevenness over 10 points. Coating density was determined by pycnometric method (DSTU ISO 2811-1:2019), through-thickness porosity and water absorption – by hydrostatic weighing (DSTU B A.1.1-49–94).

EXPERIMENTAL RESULTS AND THEIR ANALYSIS

Derived dependencies (Figure 1) allowed establishing that coating formation is influenced by the current density ratio.

In order to establish the influence of phosphates and calcium-containing components on the stages of the process of synthesis of oxide-ceramic coatings, voltage change in time was studied in electrolytes without phosphates and with their addition.

In electrolyte with 2g/l KOH + 3 g/l $Na_2O(SiO_2)_n$, initial voltages at which the coating is formed, are equal to 73–160 V (Figure 1). Here, at the stage of the first 10 min, the voltages rise faster, that is attributable to the presence of an oxide film with unipolar conductivity on the titanium alloy surface. This is exactly why this film should be removed to ensure the conditions for deposition of coatings on such alloys. In the presence of high voltages on the electrode, electron injection into the oxide layer takes place. This is what accounts for the initial voltage rise, found in all the studied systems.

The obtained results suggest that the anode voltage is influenced by the current density, which is set to be stable during synthesis. Thus, synthesizing the coating at I_a/I_c = 10/5 A/dm^2, mean voltage value at which the coating is formed, is equal to 82.5 V. If we set the

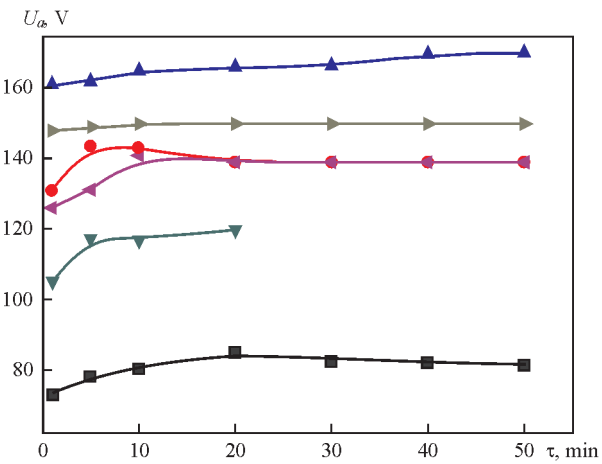

Figure 1. Electrophysical parameters of PEO-alloy Ti–6Al–4V in an electrolyte of 2 g/l KOH + 3 g/l $Na_2O(SiO_2)_n$, at current density ratios of 2, 1.5 and 1.25 and synthesis time of 20 and 50 min: ■ — I_a/I_c = 10/5 A/dm^2; ● — I_a/I_c = 75/60 A/dm^2; ▲ — I_a/I_c = 50/40 A/dm^2; ▼ — I_a/I_c = 150/100 A/dm^2; ◄ — I_a/I_c = = 150/120 A/dm^2; ► — I_a/I_c = 100/80 A/dm^2

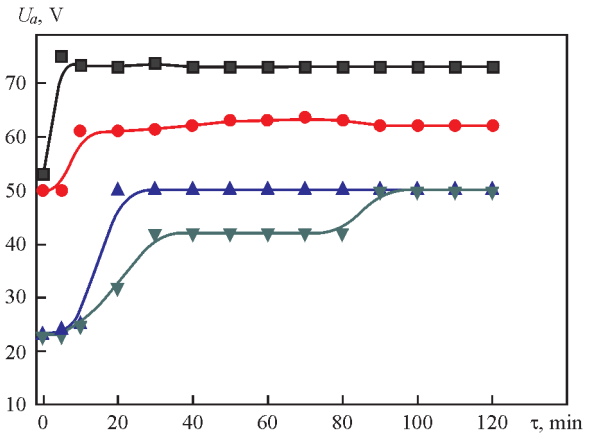

Figure 2. Electrophysical parameters of PEO-alloy Ti–6Al–4V in electrolytes of 3 g/l KOH + 2 g/l $(Na_2O(SiO_2)_n$ (■, ▲) and 5 g/l KOH + 5 g/l $(Na_2O(SiO_2)_n$ (●, ▼) at synthesis time of 120 min at I_a/I_c = 10/10 (▲, ▼) and 20/20 A/dm² (■, ●)

current density ratio I_a/I_c = 150/100 A/dm², the initial anode voltage of synthesis rises by 32 V, and the mean voltage value, at which the coating forms, rises by 35.8 V. Increase of anode current density 15 times and that of cathode 24 times (I_a/I_c = 150/120 A/dm²) leads to voltage rise at the start of synthesis by 53 V, and the mean value of voltage at which the coating forms in this mode, rises by another 3.9 V, compared to voltage of the start of PEO process in the same mode.

Note that the oxide film breakdown is followed by the process of metal oxidation in the high-temperature channel with running of plasma-chemical reactions on the anode. Such a process is represented by the rectilinear section on the curve of voltage dependence on synthesis time.

Figure 2 shows the dependencies of synthesis voltage change in phosphate free electrolytes with the ratio I_a/I_c = 10/10 and I_a/I_c 20/20 A/dm². One can see from the derived dependencies that the electrolytes with a higher concentration ensure higher

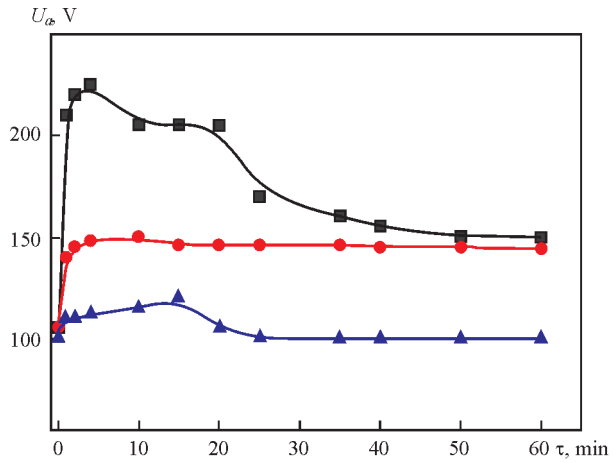

Figure 3. Electrophysical parameters of PEO-alloy Ti–6Al–4V in an electrolyte of the composition of 0.5 g/l KOH + 0.5 g/l $Ca(OH)_2$ + $Na_2O(SiO_2)_n$ + 0.5 g/l $Ca(OH)_2$ + 0.5 g/l $Na_6P_6O_{18}$ + 0.5 g/l $Na_4P_2O_7$ at I_a/I_c = 20/20 (■), 15/10 (●) and 10/10 A/dm² (▲)

conductivity, leading to decrease of voltage of the studied system.

Increase of current density leads to increase of anode voltage, electron injection into the oxide layer being provided at smaller energy losses for the breakdown channel at current density ratio I_a/I_c = 20/20 A/dm².

For coating saturation with phosphates, an electrolyte with components of sodium pyrophosphate ($Na_4P_2O_7$) and sodium hexamethaphosphate ($Na_6P_6O_{18}$) was developed. Derived dependencies of synthesis voltage change in time are presented in Figure 3.

Synthesis of oxide PEO-coatings in an electrolyte with phosphates leads to a rapid rise of anode voltage. Among the given results, we should single out the mode with current density ratio I_a/I_c = 1.5, at which uniform coatings are formed.

Having obtained the results on the dependencies at current density ratio of 15/10 A/dm³ in the electrolyte with added salts, it was found that the anode voltage coincides with the voltage, which is recorded at titanium alloy synthesis in a sodium salt free electrolyte, containing calcium hydroxide [1]. Thus, it becomes clear that sodium salts increase the conductivity of the working environment.

Coating saturation with calcium-containing components was performed through addition of hydroxyl apatite (HAp) and diatomite to the electrolyte. Electrophysical parameters of coating formation in such electrolytes are shown in Figure 4. Derived dependencies allowed establishing that the coatings form uniformly with addition of hydroxylapatite and diatomite. Thus, the developed electrolytes provide satisfactory conductivity. As one can see from the presented dependencies, oxide film breakdown in an electrolyte with HAp requires a large margin of energy which cannot be said about coating formation in an electrolyte with diatomite, where a rapid increase of anode voltage is absent. Providing a higher ratio of current density in the system, namely 20/20 A/dm², compared to 10/10 A/dm², leads to decrease of voltage, at which coating synthesis occurs, by approximately 25 V. The same regularity is preserved also for coating synthesis in an electrolyte with diatomite (Figure 4).

It should be also noted that diatomite addition to electrolyte leads to increase of electric conductivity of the working medium that reduces the anode voltage during PEO.

In order to establish the degree of hydrogen ion activity in electrolyte medium or the degree of their acidity, pH level of the medium was determined before the coating synthesis process, and after completion of the process of titanium alloy surface treatment. Thus, it was found that before the start of coating synthesis the electrolyte pH was equal to 12.6. After

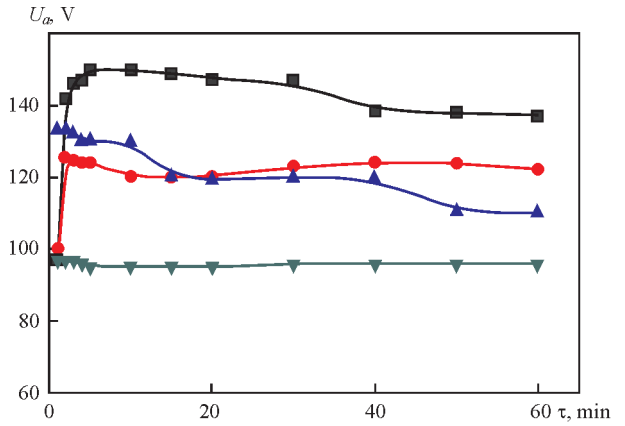

Figure 4. Electrophysical parameters of synthesis of PEO-coating on a titanium alloy in an electrolyte of 5 g/l KOH + 5 g/l $Ca(OH)_2$ + $5Na_2O(SiO_2)_n$ + 5 g/l $Ca(OH)_2$ + 5 g/l $Na_6P_6O_{18}$ + 5 g/l $Na_4P_2O_7$ + 1 g/l HAp and 20 g/l KOH + 20 g/l $Ca(OH)_2$ + + $20Na_2O(SiO_2)_n$ + 20 g/l $Na_6P_6O_{18}$ + 20 g/l $Na_4P_2O_7$ + 20 g/l diatomite: ■ — HAp with I_a/I_c = 10/10 A/dm^2; ● — HAp with I_a/I_c = 20/20 A/dm^2; ▲ — with diatomite I_a/I_c = 10/10 A/dm^2; ▼ — with diatomite I_a/I_c = 20/20 A/dm^2

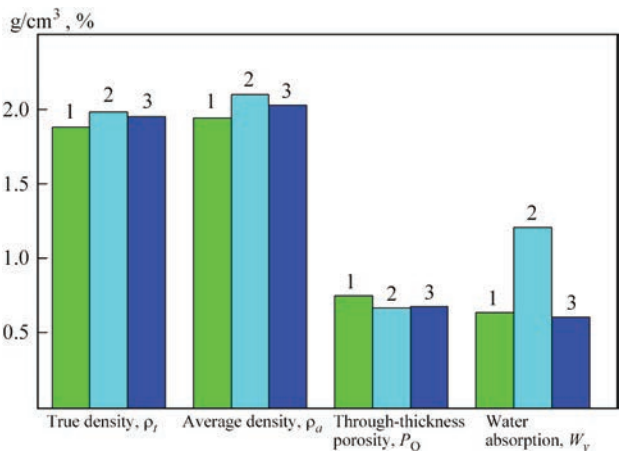

Figure 6. Results on true density, average density, porosity and water absorption of PEO-coatings synthesized in different electrolytes: *1* — 0.5 g/l KOH + 0.5 g/l l.g + 0.5$Ca(OH)_2$ + 0.5 g/l $Na_4P_2O_7$ + 0.5 g/l $Na_6P_6O_{18}$; *2* — 20 KOH + 20 g/l l.g + 1 g/l $Ca(OH)_2$ + 20 g/l $Na_4P_2O_7$ + 20 g/l $Na_6P_6O_{18}$ + 20 g/l diatomite; *3* — 3 g/l KOH + 2 g/l l.g + 3 g/l $Ca(OH)_2$

completion of the process of coating deposition on the metal surface pH level increases slightly and is equal to 12.8.

The surface of the coatings produced as a result of PEO is covered by craters and pores and it has a rather high roughness (Figure 5). This is attributable to the features of the synthesis process, which is characterized by constant formation of breakdown channels and their disappearance during the entire PEO duration. Studies of the surface morphology and its roughness revealed that the coatings synthesized in an electrolyte with diatomite (electrolyte with 20 g/l KOH + 20 g/l l.g + 20 g/l $Na_6P_6O_{18}$ + 20 g/l $Na_4P_2O_7$ + 20 g/l diatomite) have greater surface roughness (R_a = = 40 μm, R_z = 239 μm), while the coatings synthesized in electrolyte of the following composition 20 g/l KOH + 20 g/l l.g + 20 g/l $Na_6P_6O_{18}$ + 20 g/l $Na_4P_2O_7$ have roughness R_a = 5–137 μm and R_z = 28–100 μm (here l.g — liquid glass). Processing duration also influences surface roughness. So, coatings processed two times longer (60 against 30 min), have 5 times higher surface roughness. Here, owing to the twice longer processing time, surface roughness parameter R_a increases from the value of 20.4 up to 42.1 μm, while roughness parameter R_z varies from 119.7 to 239.4 μm, respectively.

Studies of the coating porosity showed that the coatings are produced with through-thickness porosity of maximum 0.75 %, that is characteristic for

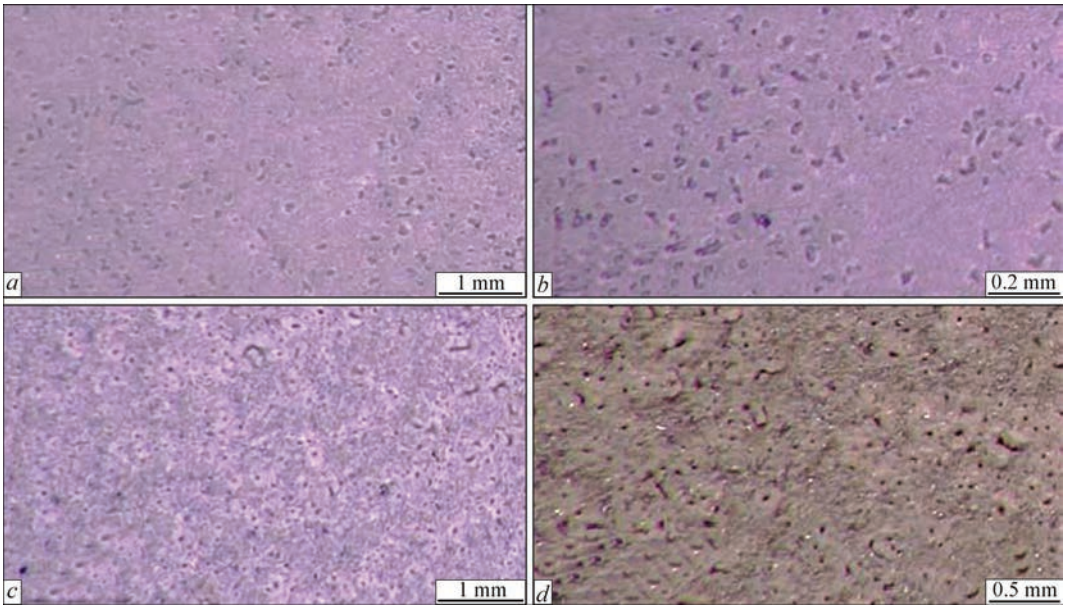

Figure 5. Surface of PEO-coatings synthesized in the following electrolytes: *a* — 5 g/l KOH + 5 g/l l.g + 5 g/l $Ca(OH)_2$ + 5 g/l $Na_6P_6O_{18}$ + 5 g/l $Na_4P_2O_7$; *b* — 5 g/l KOH + 5 g/l l.g + 5 g/l $Ca(OH)_2$ + 5 g/l $Na_6P_6O_{18}$ + 5 g/l $Na_4P_2O_7$ + 1 g/l HAp; *c* — 20 g/l KOH + 20 g/l l.g + 20 g/l $Na_6P_6O_{18}$ + 20 g/l $Na_4P_2O_7$; *d* — 20 g/l KOH + 20 g/l l.g + 20 g/l $Na_6P_6O_{18}$ + 20 g/l $Na_4P_2O_7$ + 20 g/l diatomite

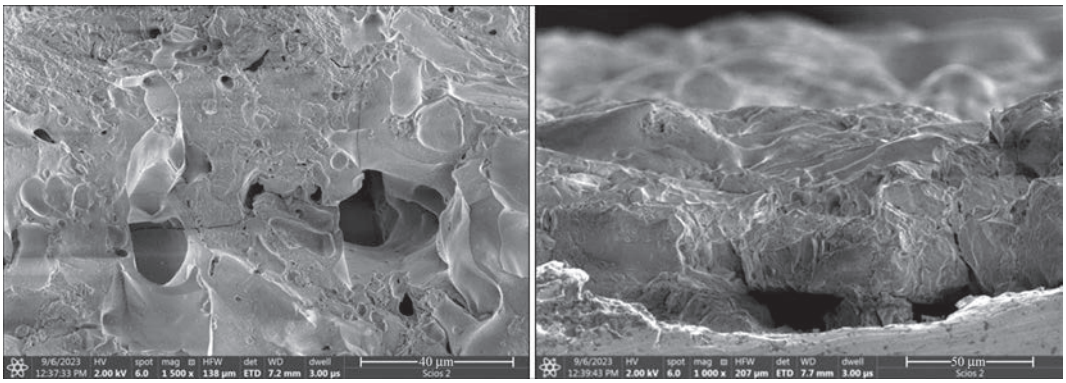

Figure 7. Fractogram of a coating at different magnifications, synthesized on a titanium alloy in the medium of 20 g/l l.g + 20 g/l KOH + 20 g/l $Na_4P_2O_7$ + 20 g/l $Na_6P_6O_{18}$ + 20 g/l diatomite at I_a/I_c = 10/10 A/dm^2, processing time of 30 min

coatings, synthesized in electrolytes with just the phosphates. Open porosity with 0.67 % values is inherent to coatings, synthesized in alkaline electrolyte of 3 g/l KOH + 2g/l liquid glass. The percentage of through-thickness porosity for coatings formed in a diatomite-containing medium decreases only slightly.

Studies of water absorption of the coatings revealed that the most porous of the mentioned coatings form in a diatomite-containing medium. Water absorption for such a kind of coatings is equal to 1.21 %, compared to coatings synthesized in electrolyte with 0.64 % phosphates, and in an alkaline electrolyte, containing just KOH and 0.61 % liquid glass.

Such results indicate that the coatings synthesized in a diatomite-containing electrolyte, are characterized by closed pores that is confirmed by fracture fractogram, shown in Figure 7.

One can see from this fractogram that pores in the coating have different dimensions, are surface melted and thus overlap. Such a result is positive as these are exactly the muscle tissues that can become embedded into the pores, leading to fast implant survival in the living body and shortening of the rehabilitation period.

CONCLUSIONS

1. The influence of the ratio of anode and cathode current density on the anode voltage was established under the conditions of biocoating synthesis by plasma electrolytic oxidation method on a titanium alloy. It was found that at I_a/I_c = 10/5 A/dm^2 in an electrolyte consisting of 2 g/l KOH + 3 g/l liquid glass, the anode voltage during PEO is the lowest, namely ~83 V, while among the selected experimental I_a/I_c ratios the highest value of anode voltage is ensured at I_a/I_c = = 50/40 A/dm^2.

2. Phosphate addition to electrolyte leads to a rapid increase of the anode voltage, which is increased twice, compared to phosphate-free electrolytes.

3. In phosphate electrolytes the coating is synthesized uniformly at the ratio I_a/I_c = 15/10 A/dm^2.

4. Addition of calcium-containing components to the electrolyte with pyrophosphate and sodium hexamethophosphate reduces the system energy consumption and stabilizes the coating formation process that is reflected in its uniformity over the entire surface.

5. Diatomite presence in the electrolyte greatly increases the conductivity of the working medium, that leads to anode voltage drop and removes the section of rapid voltage rise in the first minutes of coating synthesis, that is responsible for the breakdown of the oxide film on the titanium alloy in alkaline electrolytes, which contain only the components of potassium hydroxide and liquid glass.

6. It is found that PEO-coatings with the highest through-thickness porosity, equal to 0.75 %, form in an electrolyte of the composition of 0.5 g/l KOH + 0.5 g/l l.g + 0.5 g/l $Ca(OH)_2$ + 0.5 g/l $Na_6P_6O_{18}$ + 0.5 g/l $Na_4P_2O_7$.

7. Investigations revealed that in the coatings synthesized on a titanium alloy in an electrolyte of the composition of 20 g/l l.g + 20 g/l KOH + 20 g/l $Na_4P_2O_7$ + 20 g/l $Na_6P_6O_{18}$ + 20 g/l diatomite are characterized by a high water absorption, equal to 1.21 %, that is two times higher than this index for coatings, formed in a phosphate electrolyte and in an electrolyte without addition of other components.

REFERENCES

1. Imbirovych, N., Boyarska, I., Povstyanoy, O. et al. (2023) Modification of oxide coatings synthesized on zirconium alloy by the method of plasma electrolytic oxidation. *AIP Conf. Proc.*, 2949(**1**), 020011. DOI: https://doi.org/10.1063/5.0165655
2. Povstyanoy, O., Imbirovich, N., Redko, R. et al. (2024) *Numerical evaluation of the properties of highly efficient titanium porous materials*. Eds by V. Tonkonogyi. Advanced Manufacturing Processes InterPartner 2023. Lecture Notes in Mechanical Engineering. Springer, Cham., 307–317. DOI: https://doi.org/10.1007/978-3-031-42778-7_28
3. Duan, H., Yan, C., Wang, F. (2007) Growth process of plasma electrolytic oxidation films formed on magnesium alloy

AZ91D in silicate solution. *Electrochim. Acta*, 52(**12**), 5002–5009. DOI: https://doi.org/10.1016/j.electacta.2007.02.021
4. Tillous, K., Toll-Duchanoy, T., Bauer-Grosse, E. et al. (2009) Microstructure and phase composition of microarc oxidation surface layers formed on aluminium and its alloys 2214-T6 and 7050-T74. *Surf. Coat. Technol.*, 203(**19**), 2969–2973. DOI: https://doi.org/10.1016/j.surfcoat.2009.03.021
5. Curran, J.A., Clyne, T.W. (2005) Thermo-physical properties of plasma electrolytic oxide coatings on aluminium. *Surf. Coat. Technol*., 199(**2–3**), 168–176. DOI: https://doi.org/10.1016/j.surfcoat.2004.09.037
6. Petrosyanis, A.A., Malyshev, V.N., Fedorov, V.A., Markov, G.A. (1984) Wear kinetics of coatings made by microarcing oxidation. *Trenie i Iznos*, **5**, 350–354.
7. Student, M., Pohrelyuk, I., Padgurskas, J. et al. (2023) Influence of plasma electrolytic oxidation of cast Al-Si alloys on their phase composition and abrasive wear resistance. *Coatings*, 13(**3**), 637. DOI: https://doi.org/10.3390/coatings13030637
8. Yang, X., Ma, A., Liu, J. et al. (2019) Microstructure and corrosion resistance of yellow MAO coatings. *Surface Eng.*, 35(**4**), 334–342. DOI: https://doi.org/10.1080/02670844.2018.1445939
9. Mori, Y., Koshi, A., Jinsun Liao, J. et al. (2014) Characteristics and corrosion resistance of plasma electrolytic oxidation coatings on AZ31B Mg alloy formed in phosphate – Silicate mixture electrolytes. *Corrosion Sci.*, **88**, 254–262. DOI: https://doi.org/10.1016/j.corsci.2014.07.038
10. Nykyforchyn, H.M., Agarwala, V.S., Klapkiv, M.D., Posuvailo, V.M. (2008) Simultaneous reduction of wear and corrosion of titanium, magnesium and zirconium alloys by surface plasma electrolytic oxidation treatment. *Advanced Materials Research*, **38**, 27–35. DOI: https://doi.org/10.4028/www.scientific.net/AMR.38.27
11. Pauporté, T., Finne, J., Kahn-Harari, A., Lincot, D. (2005) Growth by plasma electrolysis of zirconium oxide films in the micrometer range. *Surf. Coat. Technol.*, 199(**2–3**), 213–219. DOI: https://doi.org/10.1016/j.surfcoat.2005.03.003
12. Timoshenko, A.V., Magurova, Yu.V. (2005) Investigation of plasma electrolytic oxidation processes of magnesium alloy MA2-1 under pulse polarisation modes. *Surf. Coat. Technol.*, 199(**2–3**), 135–140. DOI: https://doi.org/10.1016/j.surfcoat.2004.09.036
13. Zhou, H., Li, F., He, B. et al. (2007) Air plasma sprayed thermal barrier coatings on titanium alloy substrates. *Surf. Coat. Technol.*, 201(**16–17**), 7360–7367. DOI: https://doi.org/10.1016/j.surfcoat.2007.02.010
14. Shokouhfar, M., Dehghanian, C., Baradaran, A. (2011) Preparation of ceramic coating on Ti substrate by plasma electrolytic oxidation in different electrolytes and evaluation of its corrosion resistance. *Appl. Surf. Sci*., 257(**7**), 2617–2624. DOI: https://doi.org/10.1016/j.apsusc.2010.10.032
15. Stojadinovic, S., Vasilic, R., Petkovic, M. et al. (2010) Luminescence properties of oxide films formed by anodization of aluminum in 12-tungstophosphoric acid. *Electrochim. Acta*, 55(**12**), 3857–3863. DOI: https://doi.org/10.1016/j.electacta.2010.02.01
16. Snizhko, L.O., Yerokhin, A.L., Pilkington, A. et al. (2004) Anodic processes in plasma electrolytic oxidation of aluminium in alkaline solutions. *Electrochim. Acta*, 49(**13**), 2085–2095. DOI: https://doi.org/10.1016/j.electacta.2003.11.027
17. Stojadinović, S., Rastko, V., Petkovic, M., Zekovic, L. (2011) Plasma electrolytic oxidation of titanium in heteropolytungstate acids. *Surf. Coat. Technol.*, 206(**2–3**), 575–581. DOI: https://doi.org/10.1016/j.surfcoat.2011.07.090
18. Sundararajan, G., Rama Krishna, L. (2003) Mechanisms underlying the formation of thick alumina coatings through the MAO coating technology. *Surf. Coat. Technol*., 167(**2–3**), 269–277. DOI: https://doi.org/10.1016/S0257-8972(02)00918-0
19. Brewer, W.D., Bird, R.K., Wallace, T.A. (1998) Titanium alloys and processing for high speed aircraft. *Mater. Sci. and Engin.: A*, 243(**1–2**), 299–304. DOI: https://doi.org/10.1016/S0921-5093(97)00818-6 A 243(1998)299
20. Leyens, C., Peters, M. (2003) *Titanium and Titanium Alloys: Fundamentals and Applications*. Wiley-VCH, Weinheim, Germany. DOI: https://doi.org/10.1002/3527602119
21. Yao, Z.Q., Ivanisenko, Yu., Diemant, T. et al. (2010) Synthesis and properties of hydroxyapatite-containing porous titania coating on ultrafine-grained titanium by micro-arc oxidation. *Acta Biomater*., 6(**7**), 2816–2825. DOI: https://doi.org/10.116/j.actbio.2009.12.053
22. Hench, L.L. (1998) Biomaterials: A forecast for the future. *Biomaterials*, **19**, 1419–1423. DOI: https://doi.org/10.1016/s0142-9612(98)00133-1
23. Jae-Young Rho, Liisa Kuhn-Spearing, Peter Zioupos (1998) Mechanical properties and the hierarchical structure of bone. *Medical Engineering & Physics*, 20(**2**), 92–102. DOI: https://doi.org/10.1016/S1350-4533(98)00007-1
24. Dabdoub, S.M., Tsigarid, A.A., Kumar, P.S. (2013) Patient-specific analysis of periodontal and peri-implant microbiomes. *J. of Dental Research*, 92(**12**), 1685–1755. DOI: https://doi.org/10.1177/0022034513504950
25. Fakhr Nabavi, H., Aliofkhazraei, M. (2019) Morphology, composition and electrochemical properties of bioactive-TiO_2/HA on CP-Ti and Ti6Al4V substrates fabricated by alkali treatment of hybrid plasma electrolytic oxidation process (Estimation of porosity from EIS results). *Surf. Coat. Technol.*, **375**, 266–291, DOI: https://doi.org/10.1016/j.surfcoat.2019.07.032
26. Azmat, A., Asrar, S., Channa, I.A. et al. (2023) Comparative study of biocompatible titanium alloys containing non-toxic elements for orthopaedic implants. *Crystals,* **13**, 467. DOI: https://doi.org/10.3390/cryst13030467
27. Geetha, M., Singh, A.K., Asokamani, R., Gogia, A.K. (2009) Ti based biomaterials, the ultimate choice for orthopaedic implants. A review. *Progress in Mater. Sci.*, **54**, 397–425. DOI: https://doi.org/10.1016/j.pmatsci.2008.06.004
28. Zyman, Z.Z., Rokhmistrov, D.V., Glushko, V.I. (2010) Structural and compositional features of amorphous calcium phosphate at the early stage of precipitation. *J. Mater. Sci. Mater. Med*., 21(**1**), 123–130. DOI: https://doi.org/10.1007/s10856-009-3856-4
29. Furko, M., Balázsi, K., Balázsi, C. (2023) Calcium phosphate loaded biopolymer composites — A comprehensive review on the most recent progress and promising trends. *Coatings,* **13**, 360. DOI: https://doi.org/10.3390/coatings13020360
30. Colombo, P.V., Tanner, A.C.R. (2019) The role of bacterial biofilms in dental caries and periodontal and peri-implant diseases: A historical perspective. *J. Dent. Res*., 98(**4**), 373–385. DOI: https://doi.org/10.1177/0022034519830686
31. Mazinani, A., Nine, M.J., Chiesa, R. et al. (2021) Graphene oxide (GO) decorated on multi-structured porous titania fabricated by plasma electrolytic oxidation (PEO) for enhanced antibacterial performance. *Materials & Design*, **20**, 109443. DOI: https://doi.org/10.1016/j.matdes.2020.109443
32. Arash Fattah-alhosseini, Maryam Molaei, Navid Attarzadeh et al. (2020) On the enhanced antibacterial activity of plasma electrolytic oxidation (PEO) coatings that incorporate particles: A review. *Ceramics Intern.*, 46(**13**), 20587–20607 DOI: https://doi.org/10.1016/j.ceramint.2020.05.206

33. Totosko, O.V., Stukhlyak, P.D., Mykytyshyn, A.H., Levytskyi, V.V. (2020) Investigation of electrospark hydraulic shock influence on adhesive-cohesion characteristics of epoxy coatings. *Functional Materials*, 27(**4**), 760–766. DOI: https://doi.org/10.15407/fm27.04.760
34. Shu-Chuan Liao, Chia-Ti Chang, Chih-Ying Chen et al. (2020) Functionalization of pure titanium MAO coatings by surface modifications for biomedical applications. *Surf. Coat. Technol.*, **394**, 125812. DOI: https://doi.org/10.1016/j.surfcoat.2020.125812
35. Topal, E., Rajendran, H., Zgłobicka, I. et al. (2020) Numerical and experimental study of the mechanical response of diatom frustules. *Nanomaterials,* **10**, 959. DOI: https://doi.org/10.3390/nano10050959
36. Dunleavy, C.S., Golosnoy, I.O., Curran, J.A., Clyne, T.W. (2009) Characterization of discharge events during plasma electrolytic oxidation. *Surf. Coat. Tecnol*., **203**, 3410–3419. DOI: https://doi.org/10.1016/j.surfcoat.2009.05.004
37. Wang, H.Y., Zhu, R.F., Lu, Y.P. et al. (2014) Preparation and properties of plasma electrolytic oxidation coating on sand-blasted pure titanium by a combination treatment. *Mater. Sci. Eng. C. Mater. Biol. Appl*., **42**, 657–664. DOI: https://doi.org/10.1016/j.msec.2014.06.005
38. Kang, B.S., Sul, Y.T., Johansson, C.B. et al. (2012) The effect of calcium ion concentration on the bone response to oxidized titanium implants. *Clinical Oral Implants Research*, **23**, 690–697. DOI: https://doi.org/10.1111/j.1600-0501.2011.02177.x
39. Wang, M.S., Lee, F.P., Shen, Y.D. et al. (2015) Surface, biocompatible and hemocompatible properties of meta-amorphous titanium oxide film. *Int. J. of Applied Ceramic Technology*, **12**, 341–350. DOI: https://doi.org/10.1111/ijac.12184

ORCID
N.Yu. Imbirovych: 0000-0001-8276-6349,
O.Yu. Povstyanoy: 0000-0002-1416-225X,
K.J. Kurdzydlowski: 0000-0003-3875-4820,
V.V. Tkachuk: 0009-0007-1875-4774

CONFLICT OF INTEREST
The Authors declare no conflict of interest

CORRESPONDING AUTHOR
N.Yu. Imbirovych
Lutsk National Technical University
75 Lvivska Str., 43018, Lutsk, Ukraine.
E-mail: n.imbirovych@lntu.edu.ua

SUGGESTED CITATION
N.Yu. Imbirovych, O.Yu. Povstyanoy, K.J. Kurdzydlowski, V.V. Tkachuk (2024) Formation of porous coatings on titanium alloys by the method of plasma electrolytic oxidation in alkaline electrolytes saturated with phosphates and bio-additives. *The Paton Welding J*., **12**, 16–22. DOI: https://doi.org/10.37434/tpwj2024.12.03

JOURNAL HOME PAGE
https://patonpublishinghouse.com/eng/journals/tpwj

Received: 17.07.2024
Received in revised form: 20.11.2024
Accepted: 27.12.2024